

# Robust Design Optimization of a Fuel Module's Flange Aiming a Fail Safe

**Luciano Rafael Hansel Frose**  
**Rafael de Souza Almeida**  
**Gustavo Peres Mestriner**  
**José Rubens Tobias Junior**  
Robert Bosch Ltda.

**Marco Antônio Luersen**  
Federal University of Technology – Paraná

## ABSTRACT

This work presents a methodology to determine geometric dimensions of the fuel supply module flange to enhance vehicle safety by ensuring a robust component. The primary role of the fuel supply module is to supply fuel from the tank to the vehicle's injection system. In situations involving mechanical shock, it is essential for the flange and fuel module to function without enduring permanent damage. In the event of an accident or crash, the flange should break only in specific regions to prevent fuel leakage and mitigate harm to passengers. The proposed methodology relies on numerical simulations, using an initial geometry as input, and provides a comprehensive analysis of the influence of each geometric design variable. This approach results in a robust design that considers statistical variations arising from the production process.

## INTRODUCTION

Over the years, various standards have been developed to enhance vehicle safety [1]. Some of these standards focus on safety-related systems, such as ISO 26262, and improving cybersecurity, as seen in ISO 21434. Other standards aim to standardize crash types and their severity, like ISO 6813 and ISO 12353 respectively. Additionally, there are standards for testing vehicle sub-components, such as ISO 16750-3. According to ISO 39001:2012, approximately 1.3 million people lose their lives, and 20-50 million sustain injuries each year. The international community is committed to continually improving vehicle design to ensure safer transportation.

Before assessing the complete vehicle, it is possible to test individual sub-components. One such component is the fuel module, which can be tested according to ISO 16750-3. The primary function of this component is to transport fuel from the tank to the engine. It should be capable of operating without permanent failure under mechanical shock conditions. In the event of a crash, it should ideally fail in specific regions to prevent fuel leakage outside the tank,

prioritizing passenger safety. During the development of fuel modules, numerical simulation can be employed to optimize the component's geometry and ensure its robustness when subjected to various tests.

This study aims to present a methodology for parametric optimization of fuel modules using finite element simulation, which replicates test conditions. The methodology also encompasses an evaluation of the robustness of the defined optimal design.

A representative of a fuel module flange geometry, consisting of five design variables, has been defined. These variables can modify the component's geometry that connects the module reservoir with the fuel tank. Under crash conditions, this region can break off, separating the connection without allowing any fuel leakage outside the tank. Under mechanical shock conditions, the geometry should withstand accelerations without cracking. The LS-DYNA software was utilized to perform crash and mechanical shock simulations, employing explicit dynamic analysis. The optiSlang software was employed for sensitivity analysis, optimization, and robustness evaluation stages.

## FUEL SUPPLY MODULE

Figure 1 illustrates the injection system found in combustion-powered vehicles that utilize flex (i.e., gasoline and/or ethanol) or only gasoline as fuels. This system includes a fuel module responsible for capturing the fuel and employing an electric pump to transport it through line 6. Along this pathway, the fuel passes through a fine filter, effectively eliminating any residual impurities that may have remained in the tank.

Notably, the feed line always contains a surplus of fuel, exceeding the amount required for consumption. As a result, the excess fuel is redirected back to the fuel tank, ensuring continuous replenishment of the fuel module. This mechanism plays a crucial role in ensuring that the vehicle

can start even in low fuel tank conditions, as it guarantees that the fuel module remains consistently filled.

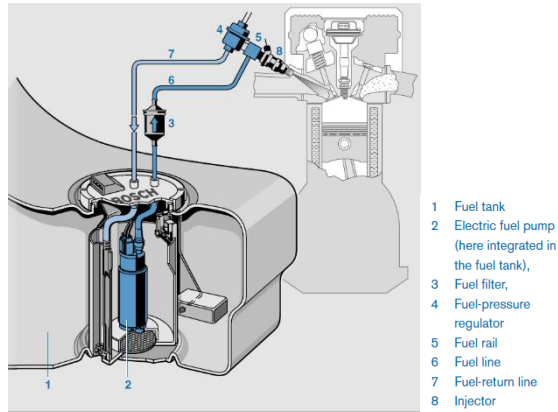


Figure 1. Injection system [2].

The fuel supply module serves two primary functions: supplying fuel at the required flow and pressure conditions throughout the vehicle's lifespan and providing accurate fuel level indication within the tank. However, these primary functions encompass a network of secondary and tertiary functions and requirements. One crucial requirement is that the fuel module must prevent any fuel leakage from the tank to the external environment under normal driving and rollover conditions. To ensure passenger safety during critical situations, various methodologies, including numerical simulations, are employed during product development.

Throughout the vehicle's operational lifespan, unforeseen events such as crashes or rollovers may occur. In such atypical circumstances, the vehicle's passengers rely on safety devices like seat belts and airbags. However, there are additional hidden mechanisms that contribute to passenger safety. One such example is the potential failure of the flange interface between the fuel tank and the WSF (Weir Sub-Frame). If a breakage occurs in the sealing area, fuel may escape from the tank. Therefore, during the WSF design process, it is imperative to simulate the connection between the rods and the flange using ISO 16750-3 parameters. This simulation aims to prevent the initiation and propagation of cracks on the sealing surface. Physically, this event can occur when the product experiences sudden acceleration while the flange remains clamped securely.

Figure 2 highlights the specific region of interest, showcasing the connection between the reservoir and the flange using a pair of connection rods with an interference fit. For clarity and enhanced comprehension, Figure 3 presents a simplified sketch that provides a clearer depiction of the pertinent components involved.

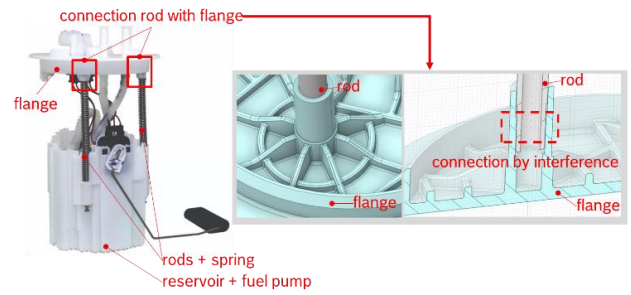


Figure 2. Region of interest in relation with complete assembly.

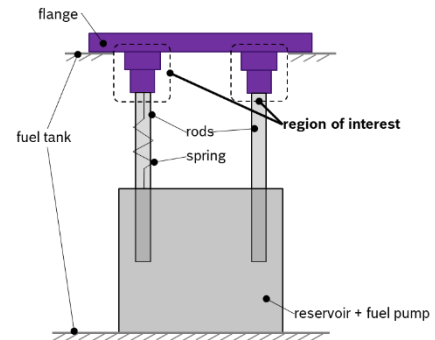


Figure 3. Simplified sketch of a fuel module.

## FUEL SUPPLY MODULE TEST REQUIREMENTS

Figure 4 depicts both crash and shock conditions. In both scenarios, the presence of a crack on the flat surface of the flange is considered undesirable. However, it should be noted that, in the case of a crash condition, a crack within the indicated region is permissible.

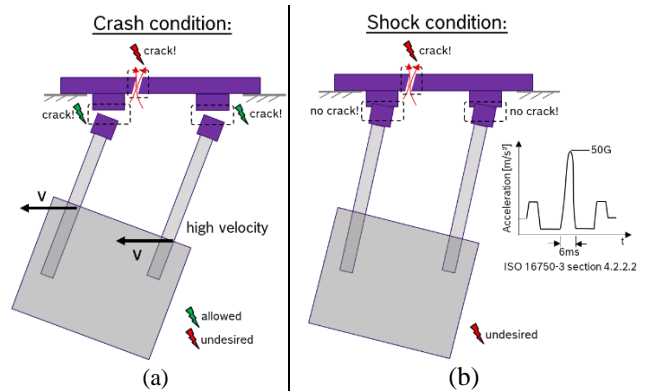


Figure 4. Crash (a) and shock (b) test conditions.

## PARAMETRIC OPTIMIZATION METHODOLOGY

Parametric optimization is a prominent category within structural optimization that aims to improve design by minimizing specific design objectives through the variation of pre-defined parameters, such as dimensions, in a model [3, 4]. This approach is particularly advantageous when

working with a well-established and validated design that already satisfies various project constraints, especially those related to manufacturing.

The initial step in formulating a parametric optimization problem is to comprehend the impact of varying the design parameters on the desired outputs. This is achieved through a sensitivity analysis, where multiple scenarios incorporating parameter variations are calculated to assess their influence on the output.

To facilitate the optimization process and reduce computational complexity, response surfaces, also known as metamodels, can be created using the calculated data points. In this study, the deep feed forward network (DFF) algorithm was employed for this purpose. Utilizing the response surface, one can proceed with the optimization problem, enabling a simpler and more cost-effective computation compared to a direct optimization approach using a finite element model. Figure 5 illustrates the difference between a direct simulation model and a metamodel. An important remark is that the metamodel output is the best possible approximation base on simulation results.

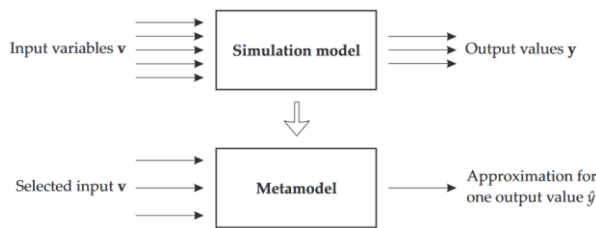


Figure 5. Simulation model approximation using metamodel [5].

Even when following this sequence of steps, it may not be sufficient to guarantee the robustness of the solution. The statistical distributions of parameters, influenced by manufacturing tolerances, can introduce variations that render deterministic optimization alone inadequate. These variations have the potential to significantly impact the results, leading to a distinct robust optimum that differs from the deterministic optimum.

To address this challenge, this paper incorporates robustness analysis in addition to multi-objective optimization considering crash and shock requirements. This analysis ensures that the optimal design not only satisfies these requirements but also accounts for statistical variations stemming from manufacturing processes.

Figure 6 illustrates how the robust design can diverge from the deterministic optimum. Robust analysis takes into consideration not only the distribution of inputs but also the distribution of responses. By doing so, it allows for a more comprehensive evaluation of the failure domain, leading to a

higher reliability compared to a deterministic optimization approach.

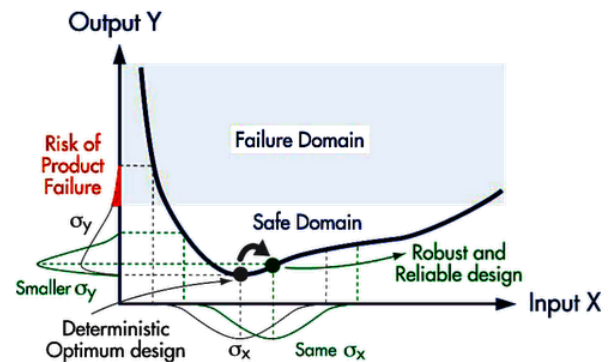


Figure 6. Deterministic vs. robust optimum design [6].

### 3D MODEL PREPARATION

A simplification of the region of interest was made and five design variables were defined. Figure 7 indicates the region of the variables and defines the fixed parameter values for the simplified flange.

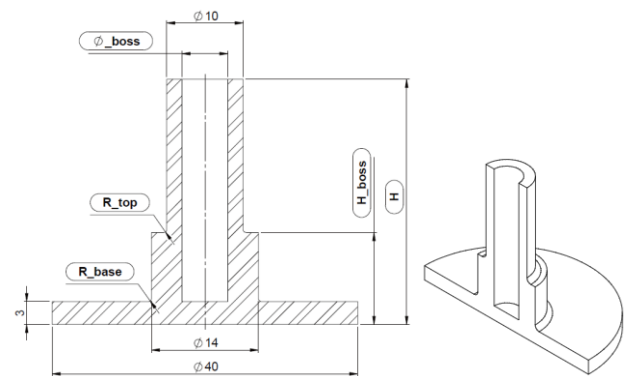


Figure 7. Simplified geometry and design variables.

The design parameters, range of variables and initial design values are shown in Table 1.

Table 1. Parameters evaluated and their respective range and initial design values.

Design parameters	Range [mm]	Initial design [mm]
R_top	0.1...1.5	0.4
R_base	0.4...1.5	0.4
$\phi_{boss}/2$	2.5...3.0	3
H_boss	10...14	12
H	30...40	32

The collected outputs are shown in Table 2. The same outputs are collected for both crash and shock simulations. The value of element erosion takes on zero value when no element is deleted and one when an element is deleted.

Table 2. Outputs collected in a simulation

Output
Element erosion @ top
Element erosion @ base
Max. principal strain @ top
Max. principal strain @ top

The Figure 8 illustrates the possible range of geometry within the design space.

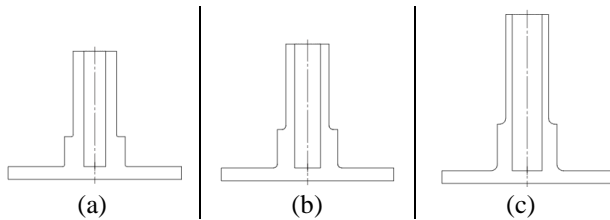


Figure 8. Comparison between ranges of design variables:  
(a) all variables at lower limit, (b) design initial, (c) all variables at upper limit.

## SIMULATION MODEL

LS-DYNA was utilized within Ansys Workbench 2023R1. To facilitate the sensitivity analysis process, Ansys Workbench was seamlessly integrated with Ansys optiSlang for further sensitivity, optimization, and robustness analysis. This coupling allowed for the execution of the flow outlined in Figure 9 for each design point. The FEA follows similar procedure from the work in [7].

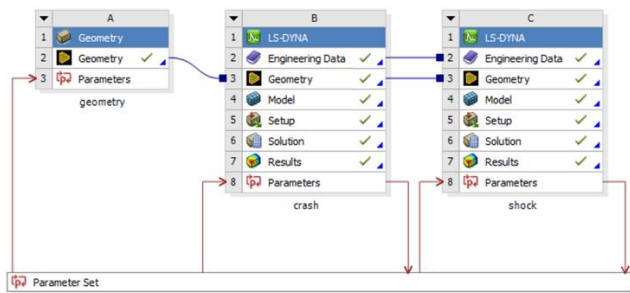


Figure 9. Workflow inside Ansys Workbench.

Figure 10 (a) indicates the boundary conditions that are used in both simulations. While for the crash simulation Fixed Support blocks all DOF in the shock simulation this region is DOF free in the Z direction. Figure 10 (b) shows the mesh used.

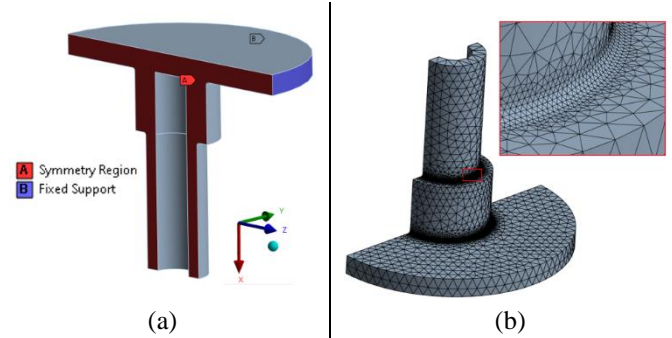


Figure 10. Boundary condition (a) and model mesh (b).

The flange material is POM with fiberglass characterized for various strain-rates. The card \*MAT\_024, \*MAT\_PIECEWISE\_LINEAR\_PLASTICITY was used to implement the material in LS-DYNA. Additionally, the card \*MAT\_ADD\_EROSION was used to implement the failure criteria. At certain known values of maximum principal stress and maximum principal strain the failure criterion is reached. Figure 11 illustrates how the stress vs strain behavior changes when the strain rate is variated. From experience it is know that failure can occur for strains higher than 0.15 mm/mm.

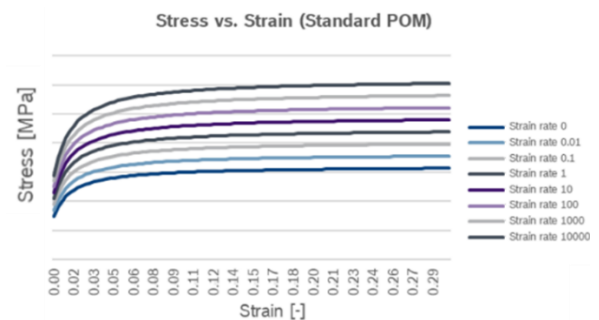


Figure 11. Stress vs. strain behavior for the flange's material for several strain rates.

## CRASH AND SHOCK ANALYSIS

The remaining boundary conditions for the crash and shock analyses are shown in Figure 12.

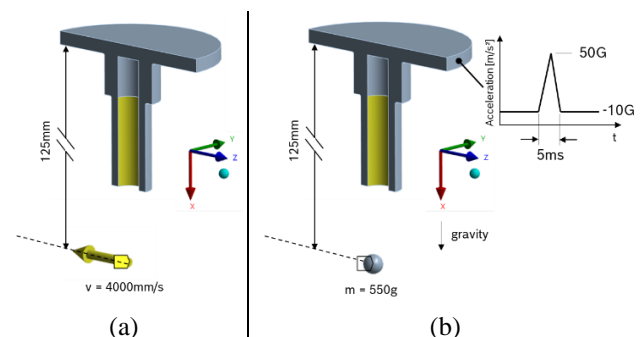


Figure 12. Boundary conditions for the crash (a) e shock (b) analyses.

The distance of 125 mm represents the distance between the flange mounting on the tank and the tank. The mass of 550g is an arbitrary representation of the mass of the tank and fuel pump assembly. Since it is a 180° symmetry, the mass value of the geometry considered would be 1100 g. The crash simulation imposes an extreme speed, with a total calculation time of 6 ms. The shock simulation, on the other hand, imposes an acceleration profile in the fixation region, with a total time of 50 ms.

## SENSITIVITY ANALYSIS

To identify which variables cannot be neglected in the optimization process, a sensitivity analysis is performed. A design is considered feasible if it meets the following requirements:

$$\text{Design space: } \begin{cases} 0.4 \leq R_{top} \leq 1.5 \text{ mm} \\ 0.4 \leq R_{base} \leq 1.5 \text{ mm} \\ 2.5 \leq \emptyset_{boss}/2 \leq 3 \text{ mm} \\ 10 \leq H_{boss} \leq 14 \text{ mm} \\ 30 \leq H \leq 40 \text{ mm} \end{cases} \quad (1)$$

Crash simulation:

subject to:  $\begin{cases} \text{erosion @ base} \leq 0 \\ \text{erosion @ top} \geq 1 \end{cases}$

Shock simulation:

subject to:  $\begin{cases} \text{erosion @ base} \leq 0 \\ \text{erosion @ top} \leq 0 \end{cases}$

In order to perform the sensitivity analysis, a metamodel was constructed. The software was configured to calculate a total of 300 points. After reaching 201 test points, the metamodel's internal quality parameters were successfully achieved, indicating that the metamodel had been successfully created. Out of the total points calculated, 107 of them met the criteria specified in Equation (1).

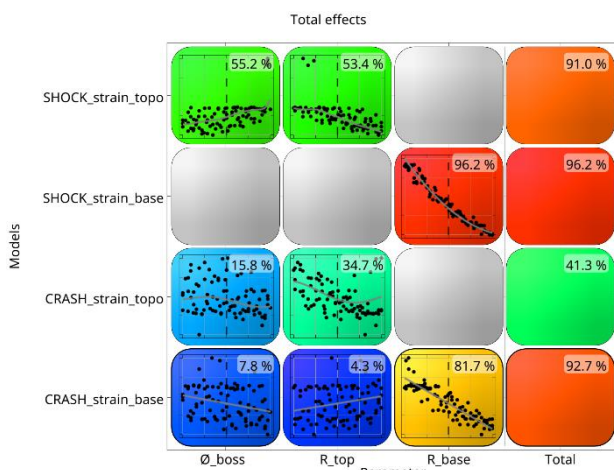


Figure 13. Sensitivity analysis results.

From Figure 13 it is possible to notice a direct correlation between the increase in  $R_{base}$  with the reduction in strain @ base, both for the shock and crash condition. The strain @ top for both test conditions is related to the  $\emptyset_{boss}$  and  $R_{top}$  variables, with  $R_{top}$  having more relevance. The variables  $H$  and  $H_{boss}$  were discarded.

It is possible to notice a direct correlation between the increase in  $R_{base}$  with the reduction in strain @ base, both for the shock and crash condition. The strain @ top for both test conditions is related to the  $\emptyset_{boss}$  and  $R_{top}$  variables, with  $R_{top}$  having more relevance.  $H$  variable was discarded from the analysis for not having great relevance according to the software criteria. The variable  $H_{boss}$  has a low correlation with the desired output and was excluded for the next steps.

Figure 14 shows the metamodel for both output locations and for both test cases. While for strain at the bottom a high coefficient of prognosis (CoP) value was achieved, strain at the top showed more nonlinearities and got a worse value, especially for crash case. Nevertheless, for strain @ top on crash case all values were higher than the limit, showing low concern on this output. Shock results are more relevant since no crack is allowed and the metamodel shows that values higher than the failure limit can occur.

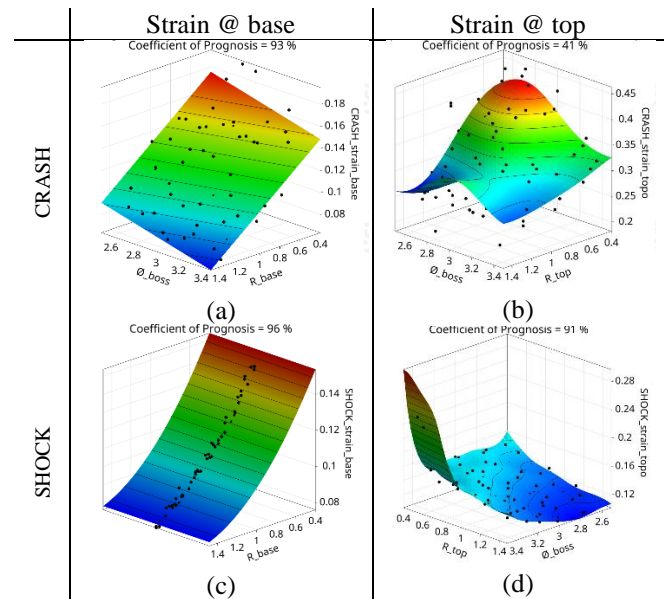


Figure 14. Metamodel generated on sensitivity analysis. (a) strain @ base for crash, (b) strain @ top for crash, strain @ base for shock and (d) strain @ top for shock.

## OPTIMIZATION PROCESS

The optimization process aims to achieve the following criteria shown in Equation (2):

$$\text{Design space: } \begin{cases} 0.4 \leq R_{top} \leq 1.5 \text{ mm} \\ 0.4 \leq R_{base} \leq 1.5 \text{ mm} \\ 2.5 \leq \emptyset_{boss}/2 \leq 3 \text{ mm} \\ H_{boss} = 12 \text{ mm} \\ H = 32 \text{ mm} \end{cases} \quad (2)$$

Crash simulation:

$$\begin{aligned} & \min\{\text{strain@base}(R_{top}, R_{base}, \emptyset_{boss})\} \\ & \max\{\text{strain@top}(R_{top}, R_{base}, \emptyset_{boss})\} \\ \text{subject to: } & \begin{cases} \text{erosion @ base} \leq 0 \\ \text{erosion @ top} \geq 1 \end{cases} \end{aligned}$$

Shock simulation:

$$\begin{aligned} & \min\{\text{strain@base}(R_{top}, R_{base}, \emptyset_{boss})\} \\ & \min\{\text{strain@top}(R_{top}, R_{base}, \emptyset_{boss})\} \\ \text{subject to: } & \begin{cases} \text{erosion @ base} \leq 0 \\ \text{erosion @ top} \leq 0 \end{cases} \end{aligned}$$

Using the metamodel generated in the sensitivity analysis, it is possible to use it for optimization, reducing the calculation time. The Figure 15 shows how the optimization process is performed within optiSlang. The solver auto-sets the "One-Click Optimization" method which evaluates several optimization algorithms and selects the most capable for the proposed activity. After performing the optimization, some validation points of the metamodel's response are analyzed for comparison.

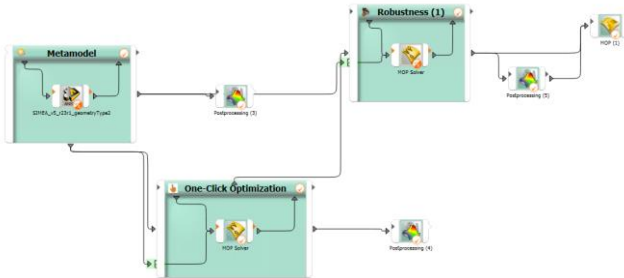


Figure 15. Optimization and robustness process using metamodel.

The multi-objective optimization results are illustrated in Figure 16 and 17. For both figures the X-axis displays the shock simulation results, while the Y-axis depicts the crash simulation outcomes. The optimum design for strain @ top (Figure 16) indicates that  $R_{top}$  should be close to its maximum value, while  $\emptyset_{boss}$  should be minimized. This approach significantly decreases the strain levels during the shock simulations while ensuring that the crash values

remain  $> 0.15$  mm/mm, allowing for the presence of cracks in the designated region.

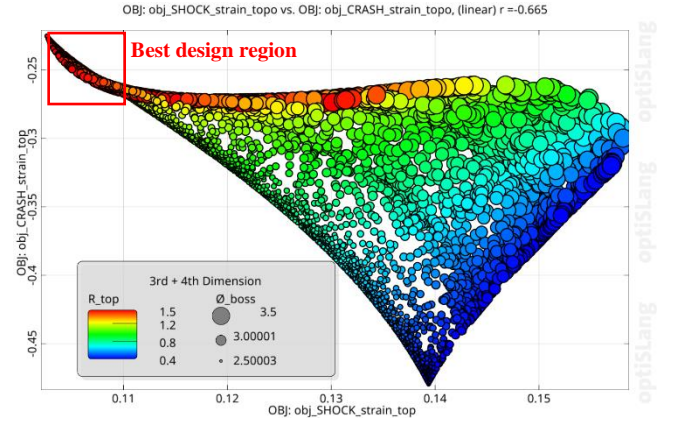


Figure 16. Strain @ top.

For strain @ base, Figure 17, the same behavior of increase radius leads to lower strain values.  $\emptyset_{boss}$  does not play a significant role since both large and small parameter values are located on the best design region.

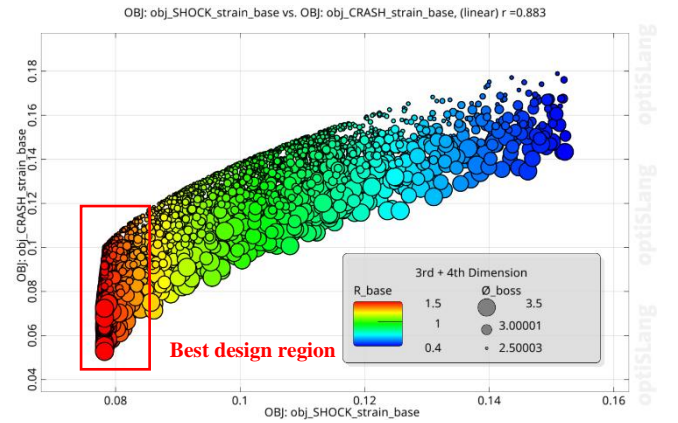


Figure 17. Strain @ base.

After performing the optimization, it was observed that  $R_{top}$  and  $R_{base}$  were found to be the most significant variables, as anticipated during sensitivity analysis. On the other hand, the variable  $\emptyset_{boss}$  was found to play a secondary role and was deemed unnecessary to include in the robustness analysis. The main goal for controlling these parameters would be to minimize their values during manufacturing. However, the tolerance range for the variable  $\emptyset_{boss}$  does not require an in-depth investigation.

## ROBUSTNESS ANALYSIS

As the final step, a robustness analysis was performed on the parameters  $R_{top}$  and  $R_{base}$  to determine the highest possible tolerance levels while ensuring a target failure

probability of 1 ppm, adhering to the principles of design for six-sigma methodology. On the robustness analysis the output distribution becomes of interest. The failure probability is then calculated based on this, as shown in Figure 18.



Figure 18. Simulation output (random response) with a safety limit (safety limit) with the design limit [8].

Figure 19 illustrates the iterative process followed for the robust design optimization. The standard deviation from the R-variables required updating for each loop. The mean value was derived from the optimal design identified through the optimization process. Table 3 presents the manual iterative design with < 1 ppm failure probability.

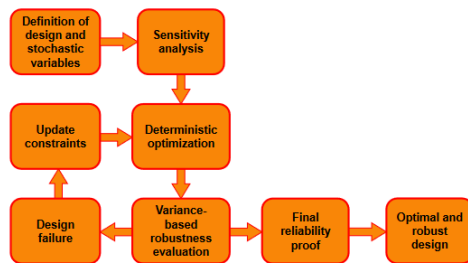


Figure 19. Iterative robust design optimization workflow [8].

Table 3. Final  $R_{top}$  and  $R_{base}$  tolerance proposal.

Parameter	Mean value	Std. dev.	Final tolerance
$R_{top}$	1.0	0.15	$1.0 \pm 0.45$
$R_{base}$	1.35	0.05	$1.35 \pm 0.15$

In Figure 20 it is possible to see a comparison between the output probability distributions. The parameter closer to the failure limit is the strain on the shock condition @ top. For the  $R_{base}$ , the crash condition is more sensible to strain variations when compared with shock.

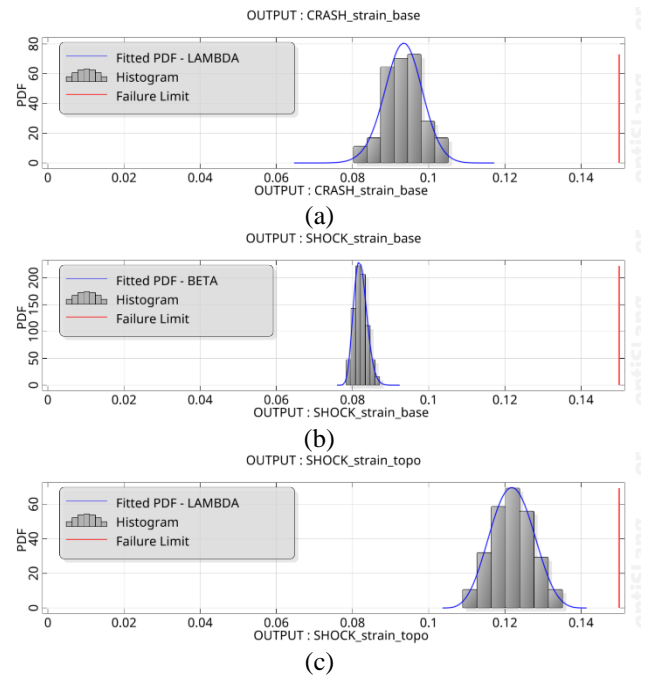


Figure 20. Output probability distribution. (a) crash condition: strain @ base. (b) and (c) shock condition: strain @ base and strain @ top respectively.

## SUMMARY/CONCLUSIONS

In summary, a robust design optimization approach was carried out for a simplified geometry of a fuel module flange. After performing a sensitivity analysis on five design parameters ( $R_{top}$ ,  $R_{base}$ ,  $H_{boss}$ ,  $H$ , and  $\varnothing_{boss}$ ), it was determined that  $H$  and  $H_{boss}$  did not significantly affect the desired outputs. The optimization process identified that larger values of  $R_{top}$  and  $R_{base}$  led to the desired outcomes while minimizing  $\varnothing_{boss}$ . The final design variables,  $R_{top}$  and  $R_{base}$ , were subjected to an iterative robust design optimization process to obtain a reliable design. The proposed tolerance ensures the design's reliability with a failure probability of <1 ppm. Overall, this study demonstrates the effectiveness of a robust design optimization approach in obtaining a reliable design for critical components in a vehicle's fuel system.

## REFERENCES

- [1] MILLER, Joseph. **Automotive System Safety**: Critical Considerations for Engineering and Effective Management. Quality and Reliability Engineering Series. Wiley, 2020. ISBN 9781119579625.
- [2] ODER, Michael *et al.* **Gasoline-engine management**: Basics and components. Robert Bosch GmbH, 2001.
- [3] ARORA, Jasbir. **Introduction to Optimum Design** (Fourth Edition). Jasbir Singh Arora (Ed.). Boston: Academic Press, 2017. iv. ISBN 978-0-12-800806-5.

[4] DE SOUZA ALMEIDA, Rafael, Ferreira, André, and Bissolatti, Marcos (2019). **Engine component development based on the application of non-parametric topology optimization**. SAE Technical Paper. doi: <https://doi.org/10.4271/2019-36-0097>.

[5] JURECKA, Florian. **Robust Design Optimization Based on Metamodeling Techniques**. 2007. Ph.D. Thesis - Technische Universität München, München.

[6] NOESIS. **Robustness & Reliability**: Engineering for the Real World. Available at: <https://www.noessolutions.com/our-products/optimus/robustness-reliability>. Accessed on: 19 may 2023.

[7] DOBES, Martin; NAVRATIL, Jiri. **Solving Crash Problems of the Fuel Supply Modules in the Fuel Tank**. In: 10th European LS-DYNA Conference 2015. Würzburg, Germany, 2015.

[8] DYNARDO GmbH. **Robust Design Optimization**. Available at: [https://library.dynardo.de/fileadmin/Material\\_Dynardo/bibliothek/WOST\\_India\\_04/01\\_Will\\_Robust\\_Design\\_Optimization\\_-\\_Overview\\_.pdf](https://library.dynardo.de/fileadmin/Material_Dynardo/bibliothek/WOST_India_04/01_Will_Robust_Design_Optimization_-_Overview_.pdf). Accessed on: 19 may 2023.

## CONTACT INFORMATION

Luciano Frose  
Rafael Almeida  
Gustavo Mestriner  
José Junior  
Marco Luersen

[luciano.frose@br.bosch.com](mailto:luciano.frose@br.bosch.com)  
[rafael.almeida2@br.bosch.com](mailto:rafael.almeida2@br.bosch.com)  
[gustavo.mestriner@br.bosch.com](mailto:gustavo.mestriner@br.bosch.com)  
[jose.junior2@br.bosch.com](mailto:jose.junior2@br.bosch.com)  
[luersen@utfpr.edu.br](mailto:luersen@utfpr.edu.br)